A Unsteady Pseudo-Compressibility Approach Based on Unstructured Hybrid Finite Volume Techniques Applied to Turbulent Premixed Flame Propagation

Wladimyr M. C. Dourado
CTA/IAE/ASA-P
São José dos Campos - 11228-904 – SP – BRAZIL
wladimyrmd@terra.com.br

João Luiz F. Azevedo
CTA/IAE/ASE-N
São José dos Campos - 11228-904 – SP – BRAZIL
azevedo@iae.cta.br

Pascal Bruel
Centre National de la Recherche Scientifique
Laboratoire de Combustion et de Détonique
BP 40109 - 86961 Futuroscope Chasseneuil Cedex FRANCE
bruel@lcd.ensma.fr

Abstract. *A method using the pseudo-compressibility technique is presented to solve the Reynolds-averaged Navier-Stokes equations for unsteady reacting flows. The combustion process is modeled using a Bray-Moss-Libby (BML) model. Turbulence closure is achieved through a two-equation $k-\epsilon$ model using classic and semi-deterministic approaches. The domain is discretized using cell-vertex, hybrid unstructured mesh techniques. To stabilize the equations, artificial dissipation is added and it is suitably modified to produce a stable system even with the adopted turbulence model. Time accuracy is recovered using an additional time derivative of conserved variables. The solution in each physical time step is obtained with a three stage Runge-Kutta scheme. The method is tested for a turbulent channel flow and the unsteady flow in the wake of a triangular bluff body. A qualitative evaluation is also carried out for the reactive case. The results present good correlation with experimental data.*

Keywords: *Turbulent flow, combustion, bluff body, finite volume method, unstructured hybrid grid, pseudo-compressibility method.*

1. Introduction

The potentialities and the use of computational fluid dynamics in our days are undoubtedly increasing both for academic research as well as for industrial application. Along the last 40 years, with help from the increase in digital computer power, more and more detailed physical phenomena and complex geometries can be investigated in our days. In this context, the present work is concerned with the simulations of turbulent combustion flows. As a large part of existing reactive flows of practical applications are in low Mach number regimes, it is necessary to choose a correct method to solve the governing equations at these conditions. On the other hand, a considerable number of numerical methods were developed in the three last decades especially for compressible flows. Hence, the pseudo-compressibility preconditioning technique appears as a good option because it results in a method only slightly different from those for the compressible regime. Furthermore, previous work (Bruel *et al.*, 1996, Corvellec, 1998, and Dourado *et al.*, 2002a) has shown that the pseudo-compressibility technique is equally efficient for structured as well as for unstructured meshes, and steady and unsteady reactive flows at very low Mach number.

On the physical side, there is a large number of models and approaches to model the combustion process and turbulence. For premixed reagent combustion cases, the model proposed by Bray *et al.* (see Bray *et al.*, 1984), has been improved and its performance is good with low computational cost. The main dependence of the combustion model success comes from the turbulent field characterization which leads to more realistically calculated combustion process. Several approaches are present in the literature for turbulence closure for the Reynolds-averaged Navier-Stokes equations. For models based in the Boussinesq hypothesis, the two-equation $k-\epsilon$ model (Jones and Launder, 1972) is one of the most popular and for some flow configurations its performance is satisfactory for separated flow. Other approaches are present in literature which seek to calculate, using $k-\epsilon$ model, unsteady separated flow, such as the semi-deterministic one, presented in the work of Ha Minh and Kourta, 1993.

The aim of the present work is to perform a validation of a numerical method to solve the Navier-Stokes equations for reacting flows, using a pseudo-compressibility preconditioning technique, on a finite volume method using hybrid unstructured meshes for spatial discretization. The present method was already validated by the authors, both for steady (see Dourado *et al.*, 2002a) and unsteady flow regimes (see Dourado *et al.*, 2002b), for

a freely propagating plane flame. The turbulence is modeled with the help of a two-equation model using both standard, or classical, and semi-deterministic approaches. The $k-\epsilon$ model proposed by Jones and Launder, 1972 is adopted and the semi-deterministic model proposed by Ha Minh and Kourta, 1993, is also considered. To model the combustion process, a Bray-Moss-Libby flamelet combustion model (see Bray *et al.*, 1984), based on a progress variable and an one step reaction with a mean reaction rate is adopted. In the present work, two test cases are considered: the entrance channel flow upstream of the bluff-body and the wake of a triangular bluff body located inside this channel. These test cases are confronted with the experimental results present in the experimental work of Sanquer, 1998. In the investigation carried out here, some integral parameters are compared with experimental data.

2. Physical Modeling

2.1. Combustion Model

The combustion model is based in the Bray-Moss-Libby model, hereafter referred to as BML model (see Bray *et al.*, 1984) for premixed combustion which assumes an isenthalpic flow with infinitely fast chemical reactions. This model gives a reaction rate for the reaction progress variable, c, which is considered to assume only two values: $c = 0$ in the unburnt mixture and $c = 1$ in the fully burnt products. This variable plays the role of a reduced temperature, i.e., $c = (T - T_r)/(T_b - T_r)$, where T_r is the temperature of the reactants and T_b is the temperature of the burnt products. With the assumptions imposed by the BML model, with the help of the heat release parameter, χ, defined as $\chi = (T_b - T_r)/T_r$, and with the use of Favre averages (Favre, 1965), the equation of state is rewritten in terms of $\tilde{c}$, the Favre averaged progress variable, as

$$\bar{\rho} = \frac{\rho_r}{1 + \chi\tilde{c}} \ . \tag{1}$$

With the hypothesis of an unitary Lewis number, the governing equation for the mean progress variable plays the role of the energy equation and it can be written in the generic form

$$L\left(\bar{\rho}\tilde{c}\right) = \bar{w} \ , \tag{2}$$

where the L operator regroups the convective and diffusive operators, and ρ is the density. The mean reaction rate, $\bar{w}$, appearing in the above equation may take different forms depending on the version of the combustion model. In the present case, $\bar{w}$, is modeled using the expression given in Bray, 1990, which take into account the intermittency, curvature and stretch of a laminar flame. This expression is written as

$$\bar{w} = \frac{1.5}{0.7}\frac{0.117\sqrt{\frac{2}{3}}}{C_\mu^{3/4}}\mathcal{K}a^{-0.784}\bar{\rho}\frac{\tilde{\epsilon}}{\tilde{k}}\frac{\tilde{c}\,(1-\tilde{c})}{1+\chi\tilde{c}} \ , \tag{3}$$

where $\mathcal{K}a$ is the Karlovitz number given as

$$\mathcal{K}a = \frac{0.157}{C_\mu^{3/8}}\left(\frac{2}{3}\right)^{3/4}\frac{\sqrt{\nu_l\tilde{\epsilon}}}{U_L^0} \ . \tag{4}$$

In above equation, U_L^0 is the non-stretched laminar flame speed and ν_l is the laminar kinematic viscosity coefficient. Other parameters are defined in the next sections. This combustion model is also detailed in Bailly, 1996, and it is adopted in this work for preliminary comparisons.

2.2. Turbulence Model

In the experimental work presented in Sanquer, 1998, all flows around the bluff body investigated have an unsteady behavior. By consequence, this flow characteristic places a more difficult requirement in the selection of turbulence model to simulate the proposed case. In some numerical investigations of flows around bluff bodies, the use of Boussinesq's approach to model the Reynolds stresses, jointly with a $k-\epsilon$ to model the turbulence parameters, gives a steady solution as presented in work of Franke and Rodi, 1991, Bailly, 1996, and Raffoul *et al.*, 1997, while other authors (see Franke and Rodi, 1991, Raffoul *et al.*, 1997, Mohammadi and Medic, 1996) show that it is possible to capture vortex shedding using this approach. A large number of these referred papers use the standard two-equation $k-\epsilon$ model given by Jones and Launder, 1972, based in the kinetic turbulent energy k and its dissipation rate ϵ. In addition, the work of Ha Minh and Kourta, 1993, Ha Minh, 1999, Billet, 1994, present an approach based in phase-averaging techniques and denominate semi-deterministic turbulence modeling or Large Eddy Simulation using time filtering. The latter authors show that, to calculate an unsteady flow, it is necessary to define a time-step small enough to capture deterministically the large structure while

Table 1: Constant values adopted for Eq. (5).

Turb. Model	C_μ (Standard)	C_μ (Semi-deterministic)	$C_{\epsilon 1}$	$C_{\epsilon 2}$	$C_{\epsilon 3}$
Standard	0.09	0.02	1.44	1.92	1.44

the small structures are modeled by the turbulence model. Thus, this rule is enforced on calculations realized in this work.

Hence, in the present work the well know two-equation turbulence model given by Jones and Launder, 1972, is adopted and written in the classical form, with the help of Favre averages (Favre, 1965) as

$$\begin{aligned}
\frac{\partial \bar{\rho}\tilde{k}}{\partial t} + \frac{\partial \bar{\rho}\tilde{u}_i\tilde{k}}{\partial x_i} &= \frac{\partial}{\partial x_i}\left(\bar{\rho}\left(\nu_l + \frac{\nu_T}{\sigma_k}\right)\frac{\partial \tilde{k}}{\partial x_i}\right) + \mathcal{P}_k - \bar{\rho}\tilde{\epsilon} + \mathcal{G}_k \ , \\
\frac{\partial \bar{\rho}\tilde{\epsilon}}{\partial t} + \frac{\partial \bar{\rho}\tilde{u}_i\tilde{\epsilon}}{\partial x_i} &= \frac{\partial}{\partial x_i}\left(\bar{\rho}\left(\nu_l + \frac{\nu_T}{\sigma_\epsilon}\right)\frac{\partial \tilde{\epsilon}}{\partial x_i}\right) + \frac{\tilde{\epsilon}}{\tilde{k}}\left(C_{\epsilon 1}\mathcal{P}_k - C_{\epsilon 2}\bar{\rho}\tilde{\epsilon} + C_{\epsilon 3}\mathcal{G}_k\right) \ ,
\end{aligned} \tag{5}$$

where k and ϵ are the turbulent kinetic energy and its dissipation rate, respectively, and $\mathcal{P}_k$ represents the turbulence production term given by

$$\mathcal{P}_k = \bar{\rho}\nu_T\left(\frac{\partial \tilde{u}_i}{\partial x_j} + \frac{\partial \tilde{u}_j}{\partial x_i}\right)\frac{\partial \tilde{u}_i}{\partial x_j} - \frac{2}{3}\left(\bar{\rho}\tilde{k} + \rho\nu_T\frac{\partial \tilde{u}_l}{\partial x_l}\right)\frac{\partial \tilde{u}_m}{\partial x_m} \ , \tag{6}$$

and $\mathcal{G}_k$ represents the turbulence production connected with the density variation. This term is modeled as present in Bailly, 1996, to validate the reactive calculations of the present work. In that reference, this term is modeled based on gradient-type hypothesis for closure such as to result in the following expression

$$\mathcal{G}_k = \frac{\tau}{\rho_r}\bar{\rho}\frac{\nu_T}{Sc_T}\frac{\partial \tilde{c}}{\partial x_i}\frac{\partial \bar{p}}{\partial x_i} \ . \tag{7}$$

where p is the static pressure, u_i and x_i are the velocity and Cartesian axis in tensorial notation, respectively.

The turbulent viscosity coefficient, μ_T, is based on dimensional analysis given by $\mu_T = \bar{\rho}C_\mu\tilde{k}^2/\tilde{\epsilon}$, with C_μ being an experimental constant. A discussion on the value of this constant as a function of approach, i.e., standard or semi-deterministic, is found in Ha Minh and Kourta, 1993, and Ha Minh, 1999. The values of the constants present in the Eq. (5) are given in Tab. 1.

3. Governing Equations

The set of governing equations is given by the Reynolds-averaged Navier-Stokes equations, with continuity equation modified by the pseudo-compressibility approach, given by (Dourado *et al.*, 2002b)

$$\frac{\partial \bar{\rho}}{\partial t} + \frac{1}{\beta}\frac{\partial \bar{p}}{\partial \tau} + \frac{\partial \bar{\rho}\tilde{u}_i}{\partial x_i} = 0 \ , \tag{8}$$

with the balance equation for reaction progress variable given by Eq. (2). Further, the two additional turbulence equations given by Eq. (5) must be considered. As presented in Dourado *et al.*, 2002a, and Bruel *et al.*, 1996, the use of the pseudo-compressibility changes the sound speed such as it is rescaled by the pseudo-compressibility parameter, β, which defines, then, a pseudo-sound speed given by

$$a = \sqrt{|u|^2 + \beta} \ , \tag{9}$$

where $|u|$ represents the magnitude of the velocity.

The governing equations are written in the standard form used for compressible, dual-time step methods for computational aerodynamics. The interested reader is referred to Dourado *et al.*, 2002a, and Dourado *et al.*, 2002b for details. Furthermore, in the present work, the turbulent transport terms, that is the Reynolds stresses, $\bar{\rho}\widetilde{u_i''u_j''}$, need a closure. For the momentum equations, the Reynolds stress tensor can be modeled based on the Boussinesq turbulent viscosity concept, by the following relation:

$$\bar{\rho}\widetilde{u_i''u_j''} = -\mu_t\left(\frac{\partial \tilde{u}_i}{\partial x_j} + \frac{\partial \tilde{u}_j}{\partial x_i}\right) + \frac{2}{3}\left(\bar{\rho}\tilde{k} + \mu_t\frac{\partial \tilde{u}_k}{\partial x_k}\right)\delta_{ij} \ , \tag{10}$$

where $\tilde{k}$ is calculated with the help of Eq. (5).

The gradient hypothesis is adopted for the term $\bar{\rho}\widetilde{u''c''}$, present in the equation for the reaction progress variable, Eq. (2), considering an analogy with Fick's law (see Bray *et al.*, 1984),

$$\bar{\rho}\widetilde{u_i''c''} = -\bar{\rho}D_t\frac{\partial \tilde{c}}{\partial x_i} \ , \tag{11}$$

where the turbulent Schmidt number Sc_t is given by $Sc_t = \nu_t / D_t$. Here, D_t is the turbulent diffusion coefficient, and the hypothesis of unitary Lewis number is adopted. Additionally to the formulation present by Dourado *et al.*, 2002a, and Dourado *et al.*, 2002b, in the present work the laminar stresses are taken into account and the laminar viscosity is calculated using Sutherland's laminar viscosity law.

4. Temporal and Spatial Discretization

The spatial discretization adopted in this work consists on an overlapped cell vertex approach, initially proposed by Mavriplis *et al.*, 1989, and adapted to hybrid unstructured grid by Dourado *et al.*, 2000, and Dourado *et al.*, 2002a, for inert and reactive flows. The physical time-depending properties, Q, and the preconditioned properties, q, are stored at the vertices of the elements. The control volume for a given vertex, i, is defined by all elements having i as a common vertex. The boundary flux integral in the governing equation is approximated, as usual in the cell vertex finite-volume formulation, using the trapezoidal rule of integration, which can be shown to be equivalent to a piecewise linear Galerkin approximation with a lumped mass matrix (see Mavriplis *et al.*, 1989). Although better shock resolution and the capture of other discontinuities, as thin flames, can be obtained using some upwind-based schemes, the present formulation is generally better suited for explicit schemes and it has lower computational cost. Further details of the numerical implementation of the spatial discretization scheme can be found in Dourado *et al.*, 2002a, and Dourado *et al.*, 2002b.

The time accurate unsteady solution of the governing equations consists in seeking a steady solution on a pseudo-time for each physical time step. The pseudo-compressibility method adopted in this work for reactive flows is based on the solution of the time-dependent Navier-Stokes equations jointly with the progress variable balance equation and the turbulence modeling equations, written in conservative form. Thus, to find the steady state within each physical time step, it is necessary to solve the discretized system of equations taking the physical time derivative as a source term, given as

$$S_T = \frac{1}{V} \int_V \frac{\partial Q}{\partial t} dV \ , \tag{12}$$

In this way, the set of discretized, coupled equations can be written as

$$V_i \frac{dq_i}{d\tau} + \left[C\left(q_i\right) - Dv\left(q_i\right) - D_a\left(q_i\right) \right] = S\left(q_i\right) - S_T\left(q_i\right) \ \ , i = 1 \ldots n. \tag{13}$$

where $C(q)$ is the residual of the convective inviscid term, $D_v(q)$ represents the viscous dissipation term and $D_a(q)$ is the artificial dissipation. V_i represents the area of the control volume i, in two-dimensional discretization.The source terms related to the reactive Navier-Stokes equations and turbulence modeling are represented by $S(q)$ and $S_T(q)$ is the physical time related source term. τ represents the pseudo-time.

In the present work, an explicit, three-stage, hybrid Runge-Kutta time-stepping scheme is adopted for time integration in pseudo-time. The reason for adopting this scheme lies with its simplicity, robustness and low computational cost which leads to the resulting scheme having an adequate performance on an unstructured grid. Thus, the scheme to advance the solution on pseudo-time step, proposed by Manzari *et al.*, 1998, is here implemented in the form

$$\begin{aligned} q_i^{(0)} &= q_i^n \\ q_i^{\kappa} &= q_i^{(0)} - \alpha_\kappa \frac{\Delta\tau}{V_i} \left[C\left(q_i^{(\kappa-1)}\right) - D_v\left(q_i^{(\kappa-1)}\right) \right. \\ &\qquad \left. - S\left(q_i^{(\kappa-1)}\right) + S_T\left(q_i^{(\kappa-1)}\right) - D_a\left(q_i^{(\kappa-1)}\right) \right], \ \text{for } \kappa = 1, 2, 3 \\ q_i^{n+1} &= q_i^{(3)} \ . \end{aligned} \tag{14}$$

Here the operators C, D_v and S are created using the properties vector $q_i^{(\kappa-1)}$ from stage $\kappa - 1$, while the artificial dissipation term is calculated only in the first stage and held constant throughout the next stages. The coefficients adopted in the Eq. (14) are: $\alpha_1 = 0.6$, $\alpha_2 = 0.6$ and $\alpha_3 = 1.0$. The physical time derivative in Eq. (12) is discretized by a second order implicit scheme given by

$$\left. \frac{\partial Q}{\partial t} \right|^{n+1,\kappa-1} = \frac{3Q^{n+1,\kappa-1} - 4Q^n - Q^{n-1}}{2\Delta t} \ , \tag{15}$$

where t represents the physical time.

This time discretization, Eq. (15), is adopted both by Rogers and Kwak, 1990, and Corvellec, 1998, on a pseudo-time marching implicit scheme context. In the present work, it was adapted in order to be used with the pseudo-time marching explicit scheme given by Eq. (14). The physical source term S is calculated at each step of the Runge-Kutta scheme above. Kunz and Lakshminarayana, 1992, present a discussion about the behavior of an explicit scheme in terms of how the source term is calculated. They conclude that this term can be calculated only in the first step of the Runge-Kutta scheme.

5. Artificial Dissipation

Since the spatial discretization adopted here can be considered a central-difference-like scheme, artificial dissipation is required to couple the equations and stabilize the system of the discretized equations. Additionally, this system needs more dissipation in the presence of high gradients such as a shock or other phenomena which could lead to unstable conditions. An appropriated fourth difference biharmonic dissipation term is added to recouple the discretized equations. The additional dissipation necessary to correctly capture shocks and/or other high property gradients is a second difference term. Thus, the adopted artificial dissipation operator used here is a blend of an undivided Laplacian and a biharmonic operator of the preconditioned properties vector q, which can be written as

$$D_a\left(q_i\right) = \sum_{k=1}^{nn} \left[\Delta_k - \Delta_i\right] \left[\frac{A_k + A_i}{2}\right] \quad , \tag{16}$$

where $\Delta(q) = k'^{(2)} q - k^{(4)} \nabla^2 q$, and nn is the number of nodes locate on the boundary of the i-th control volume. The A coefficients are added to adjust this terms for highly stretched meshes and preserve the scheme accuracy in viscous dominated regions and its form can be found both in previous work (see Dourado *et al.*, 2000, and Dourado *et al.*, 2002a) as well in Mavriplis *et al.*, 1989. Originally, the $k'^{(2)}$ coefficient was proportional to an undivided Laplacian of the pressure, which was constructed as the summation of the pressure differences along all edges defining the i-th control volume. The use of pressure as property to ponder the artificial dissipation term is logically adopted in flows with the presence of shocks. However, as the formulation adopted here is essentially for incompressible flow, this term was changed to capture high gradients of other properties. The authors observed that the proposed method became more stable when this switch is calculated as differences of k, instead of p. Equally, on semi-deterministic turbulence modeling approach, the use of ϵ as the sensor property of artificial dissipation switch is the best choice to allow the proposed scheme to be able to calculate these types of configurations evaluated here. Thus, the calculations of flow around bluff-bodies performed here use k as the sensor property and the final expression for the coefficient $k'^{(2)}$ is expressed as

$$k'^{(2)} = k^{(2)} \frac{\sum_{k=1}^{nn} |k_k - k_i|}{\sum_{k=1}^{nn} |k_k + k_i|} \quad . \tag{17}$$

For semi-deterministic calculations, k is replaced by ϵ. The constant which defines the level of fourth order dissipation $k^{(4)}$ is equal to $1/256$ for all calculations presented in this work. This value has been adequate and ideal both for compressible and incompressible schemes, giving stability, good convergence and practically no influence on the physical terms of the discretized governing equations, indicated in previous work (see Dourado *et al.*, 2002a, and Dourado *et al.*, 2002b). The $k^{(2)}$ constant defines the level of the second difference operator and numerical experiments show that its value equal to 0.05 is ideal because it produces enough dissipation on critical regions and it does not add undesirable dissipation in other regions of the computational domain. The channel flow calculations considered as test cases in the present work had this constant $k^{(2)}$ set equal to 0. For the bluff body calculations, $k^{(2)}$ was set to 0.05.

6. Test Cases Description and Boundary Conditions

A sketch of the test cases is presented in Fig. 1 with some of the main dimensions indicated. The channel flow simulated here consists of the entrance channel located upstream the obstacle. And the obstacle test case consists of whole channel flow including the entrance channel and the channel path with the obstacle. The physical height of the channel is equal to $H = 0.0288\ m$, and the obstacle base, d, have its size such that the blockage ratio, d/H, is equal to 33%. In the entrance channel test case, the inlet profiles for the longitudinal velocity component, u, for k and for ϵ are imposed using fitted polynomial equations based on the experimental data from Sanquer, 1998. The maximum velocity indicated in the experimental data at the channel axis is equal to $3.1\ m/s$. Also for this boundary, the transversal velocity component, v, is imposed equal to zero and the inlet static pressure, p, is calculated from the solution of the governing equations. The entrance test case is used to supply property profiles obtained numerically, too. Thus, for the bluff-body test case, the inlet boundary conditions for u, k and ϵ are profiles at the outlet of the entrance channel, acquired from the simulations presented here.

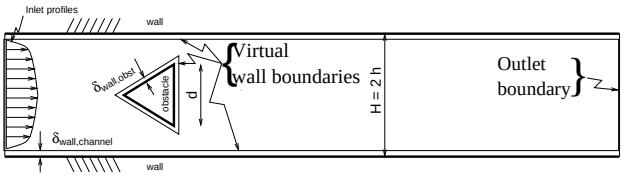

Figure 1: Sketch of obstacle test case.

The mesh near the wall is displaced from the respective actual boundaries as presented in Fig. 1, both for the entrance channel test case and the bluff-body one. For the channel wall, the virtual wall is placed away from the wall at $\delta_{wall,channel} = 0.0036\ m$ and for the obstacle wall the virtual wall is placed away from it at $\delta_{wall,obstacle} = 0.0005\ m$. The wall laws are imposed in those boundaries using the equilibrium hypothesis for turbulence production and dissipation. Further details are presented in Mohammadi and Medic, 1996. At the outlet boundary condition, the static pressure, p, is imposed and all other properties are obtained from the

Table 2: Bluff body test case designation according the turbulence model and wall law approaches used.

	Wall Law	
Approach	Logarithmic	Reichardt
Standard	**a**	**b**
Semi-deterministic	N/E	**c**

solution of the governing equations. In the reactive test case, the fuel considered is commercial propane and it is homogeneously premixed with air such that the equivalence ratio is $\phi = 0.65$. Here, U_L^0 is considered equal to $0.256\ m/s$, and $\chi = 5.15$, following Bailly's, (1996) work. In this test case, $\tilde{c}$ is imposed equal to zero in the inlet.

7. Results

7.1. Entrance Channel

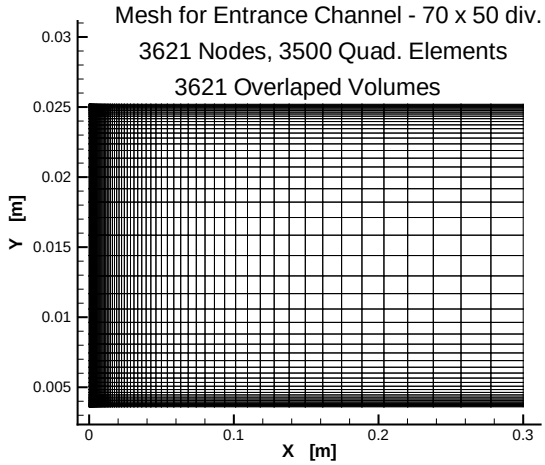

Figure 2: Mesh of entrance channel composed only by quadrangular elements.

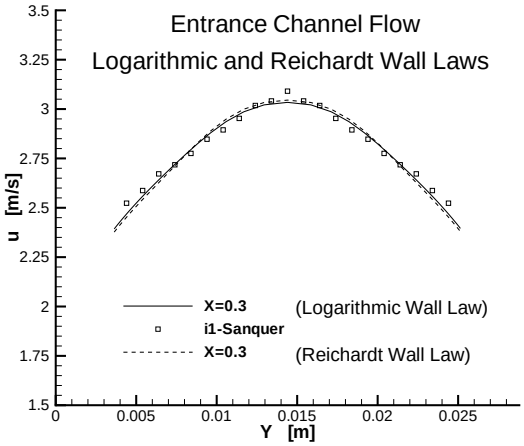

Figure 3: Mean velocity profile at channel exit and experimental results from Sanquer, 1998.

The first test case calculated with the proposed method is the entrance channel located before the bluff body and it is considered as a two-dimensional problem. This hypothesis is valid because the flow does not exhibit significant variations in the channel spanwise direction, except near the walls, as indicated by the experimental work of Sanquer, 1998. The domain is discretized using only quadrilateral elements since they produce better solutions in meshes with high aspect ratio elements as discussed in Dourado *et al.*, 2000, and Dourado *et al.*, 2002a. The adopted mesh is shown in Fig. 2. The converged solutions are achieved after almost 4000 iterations, and a single steady solution in the pseudo-time is sought. Therefore the source term of the physical time derivative in Eq. (15) is set equal to zero. The pseudo-time step, $\Delta\tau$, is calculated setting the Courant-Friedrichs-Lewis (CFL) number equal to 1.5. Both results calculated with the present method are shown in the Fig. 3 jointly with the experimental results from Sanquer, 1998. The Reynolds number based in the height of the channel, $H = 2h$, and the maximum velocity at the axis of the channel, $y = h$, is equal to 6684. The height of the channel is equal to $0.0288\ m$. It is possible to see an excellent agreement between the numerical results and the experimental data for both wall laws. This is the case named $I1$, inert, presented in Sanquer's, (1998) work. The standard turbulence model approach was used to calculated these channel flows.

7.2. Flow Around Bluff Body

The second test case consists of the flow in a channel with a triangular, equilateral, bluff body, with its vertex pointed to the entrance located at symmetry axis of the channel. The bluff body base, d, is such as to have a channel blockage equal to 33%. The mass flow is identical to the channel flow test cases. The Reynolds number based on the obstacle base size and axis velocity is equal to 2240. Two approaches for turbulence modeling were adopted to calculate this test case, the classic and the semi-deterministic as discussed in the Sec. 2.2. Two wall laws were used to calculated this test case and they are discussed in the forthcoming paragraphs. Table 2 shows the nomenclature used for each numerical case. The numerical parameters for each test case performed here for the bluff body flow are given in Tab. 3.

The mesh used to discrete the **a** and **b** test cases is shown in Fig. 4, together with the detail of the mesh around the obstacle. This is a hybrid mesh constructed with quadrilateral and triangular elements. In the entrance and exit regions of the channel, the quadrilateral element is preferable due to reasons explained before. Around the body, the strip construct by triangles with high aspect ration helps to discrete this region. Strip mesh generation procedure is a technique used by Saltel and Hecht, 1995, in their mesh generator EMC2 which

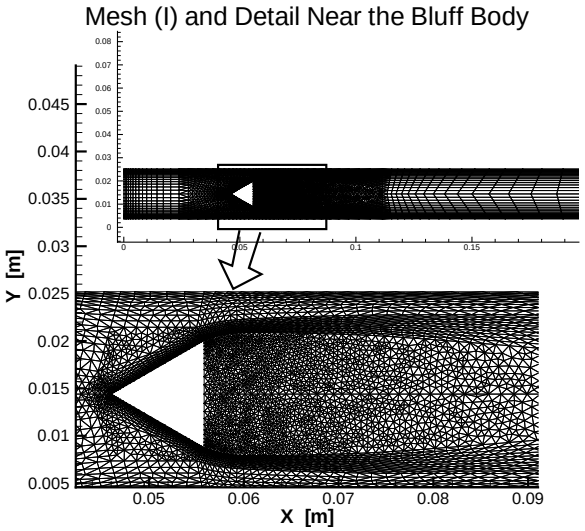

Figure 4: Hybrid mesh and detail around the triangular bluff body.

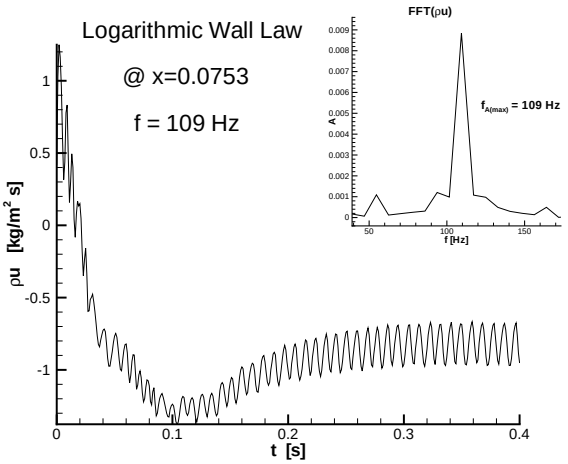

Figure 5: Component in X direction of momentum at $X = 0.07529\ m$ as function of the time using classical approach for $k - \epsilon$ model and the FTA of last $128ms$.

Table 3: Numerical parameters adopted in bluff body test case.

Case	Timestep	CFL_τ	$\Delta\tau$ calc. as func. of	Δt	Pseudo-time Conv. Criteria $\log RHS <$	$Nmax$ Iter.	Art. Dis. switch by
a	$\Delta\tau$ Const.	2	CFL_τ	10^{-4}	-4.25	3000	∇k
b	CFL_τ = const.	1.5	Spatial. var.	10^{-4}	-4.25	3000	∇k
c	CFL_τ = const.	1.3	Spatial. var.	5×10^{-5}	-4.2	3000	$\nabla \epsilon$
Reactive	$\Delta\tau$ Var.	0.5	CFL_τ	5×10^{-5}	-4.25	3000	∇k

was used to generate all grids in this work. The **c** test case needs a finer mesh than the other test case due to high gradients of k, ϵ and ν_T. The mesh for this case is a refinement of the mesh presented in the Fig. 4, for the other cases.

Numerical experiments performed in the context of the present work demonstrated that steady solutions are not possible for any of the test cases here considered. During the iteration process to seek a pseudo-time converged solution, vortex shedding appears. Obviously, they do not have any physical meaning due to the preconditioning of the equations. It should be understood that, for steady calculations, the physical time derivative is neglected, i.e., $S_T = 0$. The simulations performed here, in an attempt to obtain steady solutions, indicated that the maximum residue typically reaches values below 10^{-4} and, afterwards, starts to increase and oscillate, indicating the presence of vortex shedding. This situation is typically achieved in $3000 - 5000$ iterations in the pseudo-time marching.

Once it was clear that all computations were unsteady, the approach used in the present work was to use the calculations "converged" in the pseudo-time, in the sense described in the previous paragraph, as initial conditions for the truly unsteady simulations. For the true unsteady calculations, the convergence criterion within each physical time step was to force the logarithm of the maximum residue to be smaller than -4.25 for all control volumes. The calculations for the **a** case were performed up to the physical time of 400 ms and the history of the momentum component in longitudinal direction along the axis of the channel, at $X = 0.07529$ which correspond the experimental length of the recirculation zone is presented in Fig. 5. In the same figure, the Fourier temporal analysis (FTA) of the last 128 ms is plotted. The vortex shedding frequency found is equal to $f = 109\ Hz$. This result indicates a Strouhal number $St = fd/U_{axis}$ equal to 0.3375. In the experimental data, the Strouhal number is equal to 0.276.

In Fig. 6, contours of mean velocity magnitude and streamlines for six different instances in a given period are shown. In Fig. 7 the evolution of the mean longitudinal velocity component along the axis of the channel, behind the back face of the obstacle, is presented. This face is locate at $X = 0.0558\ m$ and the end of the recirculation

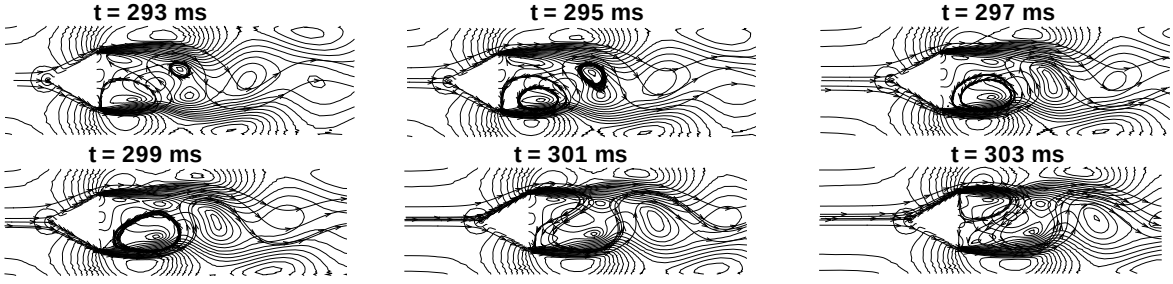

Figure 6: Mean velocity magnitude and streamline at six times in a period of 87 Hz.

Table 4: Bluff body test case integral parameters.

	$f\ [Hz]$	fd/U_{axis}	$X_L\ [m]$	$\Delta X_L\ [m]$	$\Delta X_L/d$
Std. Turb. Model w/ Log. WL	109	0.3375	0.0789	0.0231	2.41
Std. Turb. Model w/ Reichardt WL	87	0.2694	0.078	0.0222	2.31
Semi-Determ. w/Reichardt WL	161	0.4986	0.0719	0.0161	1.68
Experimental (Sanquer, 1998)	89	0.276	–	0.0204	2.12

zone is achieved at $X = 0.0789\ m$. It results in a length of the recirculation zone equal to $\Delta X_L = 0.02313\ m$. Table 4 summarizes the integral parameters for bluff body test case calculated here with the present method.

The history of the longitudinal component of momentum during 305 ms of calculations of the **b** case at $X = 0.07529\ m$ is plotted in Fig. 8. The improvement of the main frequency of vortex shedding calculations can be observed as shown in Tab. 4. The results in this case are essentially equal to the experimental data. The present work confirms the expectation of Strouhal number improvement using a more sophisticated wall law as suggested by Mohammadi and Medic, 1996. A better mean value is also obtained in the evolution of mean longitudinal velocity component at axis of the channel, behind the obstacle, using the Reichardt wall law and standard approach for $k-\epsilon$ model, shown in Fig. 9. Based on the results presented in this figure, it is possible to find the dimensionless length of recirculation zone as equal to 2.31, which is 9% larger than the experimental. Hence, this indicates a fairly good agreement between the calculations performed with the present method and the experimental data.

The proposed method was also used to test an other approach, called "semi-deterministic" modeling. The history of the velocity component in the X direction along the axis of the channel, behind the obstacle is shown in Fig. 10.The frequency of vortex shedding in this cases is equal to 161 Hz. This value is completely different from the experimental and the other numerical results. Although the velocity component along the axis of channel has a very dispersive character in time, the mean velocity profile keeps the shape of the **a** and **b** cases, with the dimensionless length of recirculation zone equal to 1.68. Some values assumed in some given times and the temporal mean value are presented in Fig. 11. The results using semi-deterministic approach performed here has been deteriorated in comparison with the classical one, in opposition to the improvement obtained by Ha Minh and Kourta, 1993.

Finally, a short test was performed for a reactive case to evaluate the ability of the present method to model turbulent unsteady reacting flow. The temperature distribution in a given physical time is shown in Fig. 12, where the calculation was performed using the BML reaction rate expression defined at Eq. (3) is adopted. Although the geometry of the obstacle used in the test cases calculated by Bailly, 1996, is different, the preliminary results obtained in present study are encouraging. The method is able to calculate higher temperatures at the near wake of the obstacle and the unsteady behavior is equally present. The authors believe that the temperature increase before the obstacle is the result of the numerical diffusion of the progress variable, which suggests the need for further mesh refinement studies in the future work. The mesh used for this reactive case is precisely the same one used for the **a** and **b** cases, shown in Fig. 4.

8. Concluding Remarks

A time-accurate coupled explicit procedure for solving the unsteady reacting Navier/Stokes equations was presented and tested on two basic test cases: a channel flow and the wake of a triangular bluff body. Some observations are possible considering the results here discussed. First, the adopted two-equation turbulence model gives good results for some integral parameters there are in good agreement with experimental data. The mean velocity along the channel flow test case has agreed with experimental results for both logarithmic wall law as well as the Reichardt wall law. The length of the recirculation zone has a fair agreement with experimental data when the baseline $k-\epsilon$ model with the logarithmic wall law is adopted. Improvement in Strouhal number and length of the recirculation zone are obtained with the use of Reichardt wall law. Second, the semi-deterministic approach for the two-equation model results on degradation of the integral parameters, mainly the Strouhal number. The length of the recirculation zone does not agree well with the experimental data either.

The authors believe that the good results obtained with the present method using the classical approach for turbulence modeling are a consequence of good spatial resolution with reduced numerical diffusion. As a consequence, the unsteady flows were well captured. The use of the Laplacian of one of the turbulence properties, k or ϵ, to switch the second difference artificial dissipation term is able to stabilize the numerical method even in the presence of the high Reynolds number $k-\epsilon$ model. For the semi-deterministic approach, only the use of the Laplacian of ϵ makes the discretized system of equations stable.

A qualitative evaluation of the present method in unsteady reactive calculations is performed and it shows that the method is robust enough to calculate such combustion flows. The reactive case calculations seem to indicate a better correlation with the expected results, which is an improvement over similar simulations

available in the literature. Moreover, further investigations of the semi-deterministic approach is necessary as well as more detailed validation of the reactive case.

9. References

Bailly, P., 1996, "Contribution to the Study of Turbulence-Combustion Interaction in Premixed Turbulent Flames with Help of Second Order Models", Ph.D. Thesis, Université de Poitiers.

Billet, G., 1994, "Turbulent Realizability Conditions for a Semi-Deterministic Method to Simulate a Supersonic Mixing of a Hot Jet in a Co-Flowing Stream and Comparison With Experimental Data," *1994 ICHMT - International Sumposium on Turbulence, Heat and Mass Transfer*, No. 1994-84, ONERA, France.

Bray, K. N. C., 1990, "Studies of the Turbulent Burning Velocity," *Proceeding of the Royal Society of London*, Vol. A 431, pp. 315–335.

Bray, K. N. C., Libby, P. A., and Moss, J. B., 1984, "Flamelet Crossing Frequencies and Mean Reaction Rates in Premixed Turbulent Combustion," *Combustion Science and Technology*, Vol. 41, pp. 143–172.

Bruel, P., Karmed, D., and Champion, M., 1996, "A Pseudo-Compressibility Method for Reactive Flows at Zero Mach Number," *International Journal of Computational Fluid Dynamics*, Vol. 7, pp. 291–310.

Corvellec, C., 1998, "Numerical and Analytical Study of a Combustion Zone Propagating Characteristics Developing on Premixed Turbulent Flow Modelized by a Flamelet Approach Type", Ph.D. Thesis, Université de Poitiers.

Dourado, W. M. C., Azevedo, J. L. F., and Bruel, P., 2000, "Application of the All-Speed Method to Steady and Unsteady Flows on Unstructured Grids," *Proceedig of the 8th Brazilian Congress of Thermal Engineering and Sciences*, Porto Alegre, RS, Brazil.

Dourado, W. M. C., Azevedo, J. L. F., and Bruel, P., 2002a, "A Steady Pseudo-Compressibility Approach Based on Unstructured Hybrid Finite Volume Techniques Applied to Turbulent Premixed Flame Propagation," *9th Brazilian Congress of Thermal Engineering and Science"*, Caxambu, MG, Brazil.

Dourado, W. M. C., Bruel, P., and Azevedo, J. L., 2002b, "A Time-Accurate Pseudo-Compressibility Approach Based on Unstructured Hybrid Finite Volume Technique Applied to Unsteady Turbulent Premixed Flame Propagation," paper submited to the *International Journal for Numerical Methods in Fluids.*

Favre, A., 1965, "Compressible Turbulent Gas Equations," *Journals de Mécanique*, Vol. 4, pp. 361–391.

Franke, R. and Rodi, W., 1991, "Calculation of Vortex Shedding Past a Square Cylinder with Various Turbulence Models," *8th Symposium on Turbulent Shear Flows*, No. 20-1, pp. 20–1–1/20–1–6, Univ. of Munich.

Ha Minh, H., 1999, "La Modelisation Statistique de la Turbulence: ses Capacites et ses Limitations," *C. R. Academie des Science de Paris*, Vol. 327, No. II b, pp. 343–358.

Ha Minh, H. and Kourta, A., 1993, "Semi-Deterministic Turbulence Modelling for Flows Dominated by Strong Organized Structures," *9th Symposium on Turbulent Shear Flows*, number 10-5. Kyoto.

Jones, W. P. and Launder, B. E., 1972, "The Prediction of Laminarization with a Two-Equation Model of Turbulence," *International Journal of Heat and Mass Transfer*, Vol. 15, pp. 301–314.

Kunz, R. F. and Lakshminarayana, B., 1992, "Stability of Explicit Navier-Stokes Procedures Using $k-\epsilon$ and $k-\epsilon$/Algebraic Reynolds Stress Turbulence Models," *Journal of Computational Physics*, Vol. 103, pp. 141–159.

Manzari, M. T., Hassan, O., Morgan, K., and Weatherill, N., 1998, "Turbulent Flow Computation on 3D Unstructured Grids," *Finite Elements in Analysis and Design*, Vol. 30, pp. 353–363.

Mavriplis, D. J., Jameson, A., and Martinelli, L., 1989, "Multigrid Solution of the Navier-Stokes Equations on Triangular Meshes," NASA CR-89-11, ICASE, NASA Langley Research Center, Hampton, VA.

Mohammadi, B. and Medic, G., 1996, "A Critical Evaluation of the Classical $k-\epsilon$ Model and Wall-Laws for Unsteady Flows over Bluff Bodies," Research Report No. 3056, INRIA, Rocquencourt, France.

Raffoul, C. N., Nejad, A. S., Gould, R. D., and Spring, S. A., 1997, "An Experimental and Numerical Study of the Isothermal Flowfield Behind a Bluff Body Flameholder," *Trans. of the ASME*, Vol. 119, No. 2, pp. 328–339.

Rogers, S. E. and Kwak, D., 1990, "An Upwind Differencing Scheme for the Time-Accurate Incompressible Navier-Stokes Equations," *AIAA Journal*, Vol. 28, No. 2, pp. 253–262.

Saltel, E. and Hecht, F., 1995, "EMC2 Wysiwyg 2D finite elements mesh generator," Tech. Rep. No. 118, INRIA, France.

Sanquer, S., 1998, "Experimental Study of a Buff-Body Wake, in Presence of Combustion, in Fully Developed Turbulent Channel Flow: Turbulence Scales and Critical Analysis of Transport and Combustion Models", Ph.D. Thesis, Université de Poitiers.

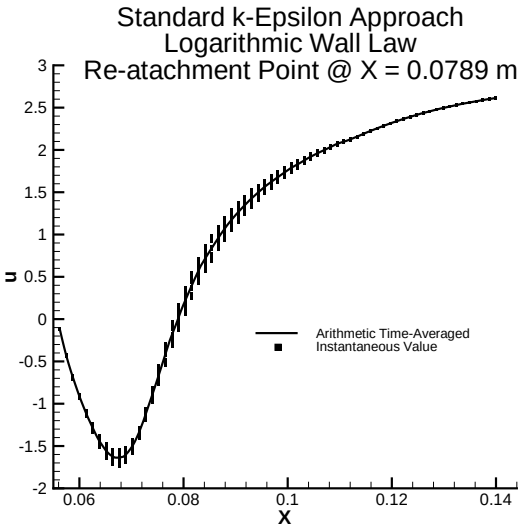

Figure 7: Axial evolution of mean longitudinal velocity component using logarithmic wall law and standard $k-\epsilon$ model.

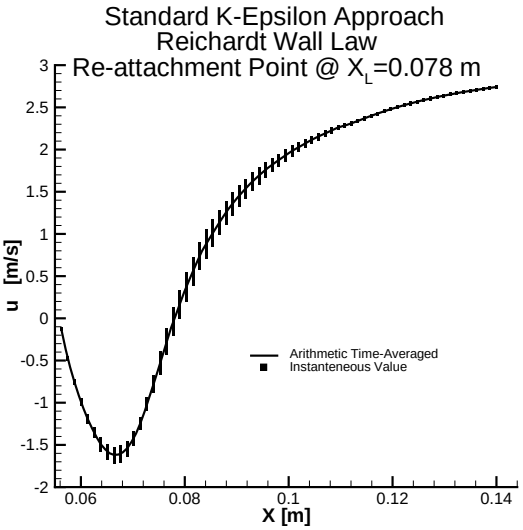

Figure 9: Axial evolution of mean longitudinal component velocity using Reichardt wall law and standard approach for $k-\epsilon$ model.

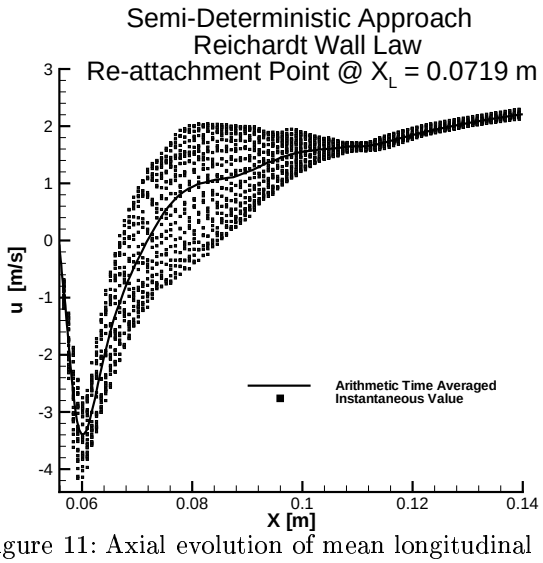

Figure 11: Axial evolution of mean longitudinal component velocity using Reichardt wall law and semi-deterministic approach for $k-\epsilon$ model.

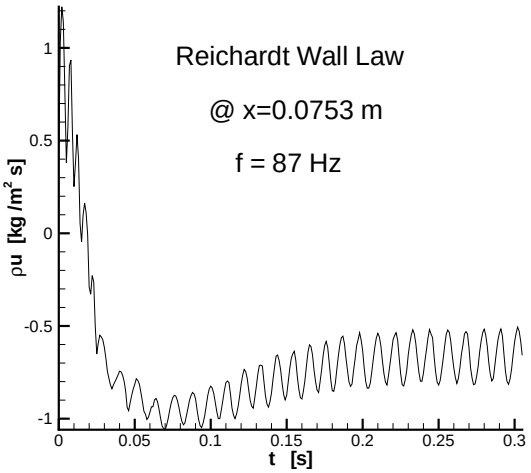

Figure 8: Component in X direction of momentum at $X = 0.07529\ m$ as function of the time using Reichardt wall law and standard approach for $k-\epsilon$ model.

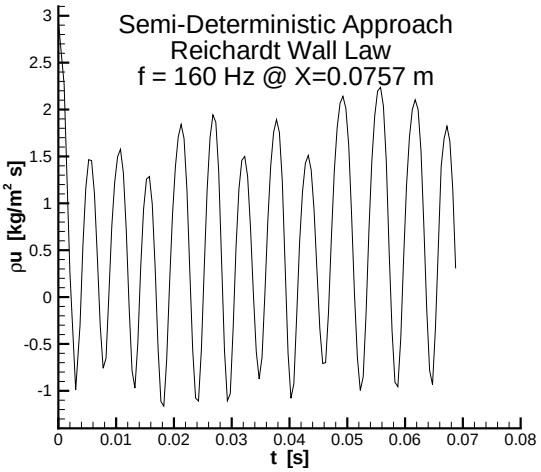

Figure 10: Component in X direction of momentum at $X = 0.07567\ m$ as function of the time using Reichardt wall law and semi-deterministic approach for $k-\epsilon$ model.

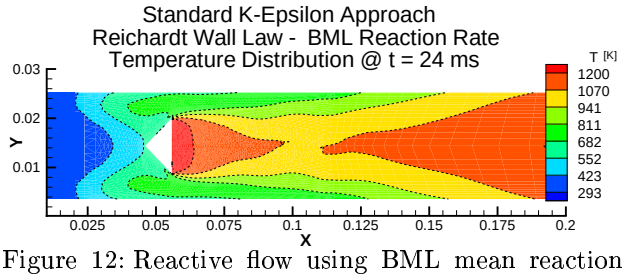

Figure 12: Reactive flow using BML mean reaction rate for the progress variable: temperature contours.